ELSEVIER

Theoretical and Applied Fracture Mechanics 30 (1998) 65–73

theoretical and applied fracture mechanics

Effect of stress ratio and specimen thickness on fatigue crack growth of CK45 steel

J.D.M. Costa *, J.A.M. Ferreira

Department of Mechanical Engineering, University of Coimbra, DEM/FCTUC, Pinhal de Marrocos, 3030 Coimbra, Portugal

Abstract

Presented are the effect of stress ratio and thickness on the fatigue crack growth rate of CK45 steel according to DIN 17200. Test results are obtained for constant amplitude load in tension with three stress ratios of $R = 0$, 0.2 and 0.4 and three specimen thicknesses of $B = 6$, 12 and 24 mm. Microgauge crack opening values were used to calculate ΔK_{eff} values from which the $\mathrm{d}a/\mathrm{d}N - \Delta K_{\text{eff}}$ curves are obtained. Crack closure can be applied to explain the influence of mean stress and specimen thickness on the fatigue crack growth rate in the second regime of the two-parameter crack growth rate relation. An empirical model is chosen for calculating the normalized load ratio parameter U as a function of R, B and ΔK and, for correlating the test data.

1. Introduction

Crack closure has played a central role in the study of fatigue crack propagation [1]. A large number of researchers have made attempts to understand the influences of mean stress [2,3] and specimen thickness [4,5] on the fatigue crack growth rate based on the crack closure argument. These influences, however, were not always attributed to the crack closure phenomenon [6]. The reasons for such misdirected implications are partly due to the lack of measurement accuracy and/or improper experimental techniques when determining the crack closure.

Cause of crack closure [7] has been attributed to plasticity, oxidation and surface roughness. Except for high stress ratios or high ΔK values, fatigue crack growth can be affected by crack closure due to plasticity in the two-parameter crack growth rate relation, Regime II and by oxidation and surface roughness in Regime I of the two-parameter crack growth rate relation. The influence of mean stress on the fatigue crack growth rate in the former case has been explained by crack closure using the normalized load ratio parameter U as a function of R alone [3,8]; of R and $K_{\max}$ [9]; and of R and ΔK [10]. Sometimes, U tends to increase with R and decrease with increasing $K_{\max}$ [11,12]. This, however, is in contrast with the conclusion in Ref. [9] that U increases with $K_{\max}$.

Two different specimen thicknesses $B = 0.3$ and 6.35 mm were used to study the crack growth rate [13] for two different steels (1018 and 9CK–lMo) and three aluminium alloys (2024, 6061 and IN9021). Specimen thickness influence on the crack rate growth were not present for the 1018 steel and 2024 and 6061 aluminium alloys. Thickness effects observed for the 9Cr–lMo and IN9021 alloys were attributed to the pronounced contraction at the lateral surfaces near the crack

* Corresponding author. Tel.: +351 39 790 700; fax: +351 39 790 701; e-mail: jose.domingos@mail.dem.uc.pt.

0167-8442/98/$ – see front matter
PII: S0167-8442(98)00044-5

tip. A reduction in ΔK_{eff} thus prevails. Surface contractions for these two materials were obtained. Specimen thickness variation had little influence on U. But for values below certain critical thickness B_c, the U parameter was very sensitive to thickness variations.

Three different thicknesses of compact tension specimens were tested in fatigue for three stress ratios values. The objectives of this work are to measure the crack length and crack closure for fatigue; to analyze the crack closure variation with K_{max}, (or ΔK), for different R and B values; to obtain the $da/dN - \Delta K_{eff}$ curves such that the influences of B and R could be eliminated; and to propose an empirical model that could correlate U with R, B and ΔK.

2. Experimental considerations

Chemical composition and the mechanical properties of CK45 (DIN 17200) steel, are shown in Tables 1 and 2, respectively.

Fatigue tests were conducted for the compact tension (CT) specimens with three different thicknesses: $B = 6$, 12 and 24 mm according to the ASTM E647 standard [14]. The specimens were obtained in the transverse longitudinal direction from a laminated bar with rectangular section 30×60 mm^2. The tests were performed in a load-controlled servohydraulic INSTRON (model 1341) machine with 100 KN of capacity. The load is constant amplitude with a frequency of 20 Hz. Optical and direct current potential drop were used to measure the crack length. The specimens were machined and polished mechanically.

Table 1
Chemical composition of CK45 (DIN 17200) steel

C (%)	Si (%)	Mn (%)	P (%)	S (%)
0.42–0.50	0.15–0.35	0.50–0.80	0.035	0.35

Table 2
Mechanical properties of CK45 (DIN 17200) steel

σ_r (MPa)	σ_c (MPa)	ε_r (%)	Hardness HB
670–820	420	>16	205

The optical measurements were made in travelling microscope (30X) with an accuracy of 10 μm. The direct current potential drop (DCPD) method consists of a power supply KEPCO, (model A-TE6-50) (with 0–50 A) and a microvoltimeter RACAL DANA (model 5001) with 1 μV of resolution. During the tests, the current was constant in the range 30–50 A. Note that 30 A were used for thickness $B = 6$ mm, and 50 A for $B = 24$ mm. The measurements of the DCPD were in the range 150–2000 μV from the start until the end of the test. The cables that conducted the current to the specimens were connected by using two treaded bolts at the top and bottom surfaces of the specimens. The DCPD was obtained by two electrical conductors of nickel with 0.1 mm of diameter welded by the resistance welding process. The machine used to perform the welds was a Shandon model Elliot.

Crack closure measurements (opening loads) were made using a Elber type gauge [1] near the crack tip located above and below the crack surfaces where two holes of 0.5 mm diameter were drilled for the gauge pins. The distance between these points was 1.2 mm and about 1 mm from the crack tip. The load–displacement records were obtained at a frequency of 0.2 Hz.

At the start of this series of tests, other types of crack closure measurement techniques were attempted namely, the Crack Mouth Gauge and the DCPD technique. In both cases, the results indicated that these transducers are not adequate due to insufficient sensibility. In the case of the DCPD technique, the load–displacement records did not correlate with the crack closure phenomenon.

From the load–displacement records, variations of the opening load P_{op} were derived using the point where the curve begins to be linear during the loading part of the cycle as shown in Fig. 1. The parameters U, K_{op} and ΔK_{eff} are given by the expressions:

$$U = (P_{max} - P_{op})/(P_{max} - P_{min}), \tag{1}$$

$$K_{op} = K_{max} - U\Delta K, \tag{2}$$

$$\Delta K_{eff} = U\Delta K. \tag{3}$$

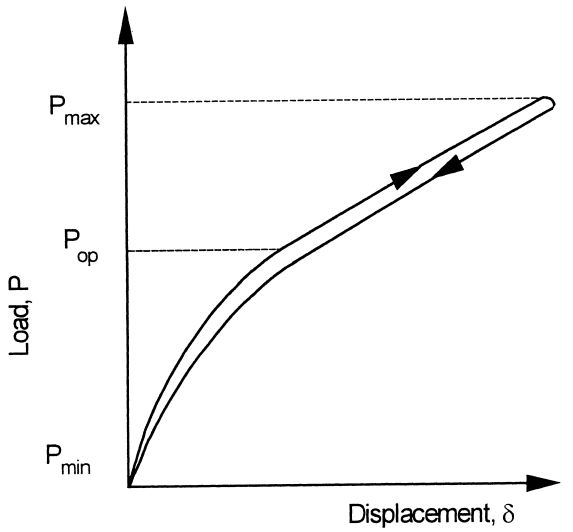

Fig. 1. Schematic presentation for the determination of the opening load, P_{op}.

3. Results and discussions

Table 3 shows some U expressions for past models. Most of them consider U as a function of R only. Other models treat U as function of R and ΔK or K_{max}. However, none of them include the influence of specimen thickness.

3.1. Mean stress and specimen thickness

The influence of stress ratio on fatigue crack growth can be seen from Fig. 2(a) for $B = 6$mm and $R = 0$, 0.2 and 0.4. Strong influence of the stress ratio on fatigue crack growth rate is observed. As ΔK increases, the influence of R on da/dN decreases. The crack growth rate da/dN increases with R; this trend is more pronounced between $R = 0$ and 0.2 than that between $R = 0.2$ and 0.4. For high values of da/dN near 10^{-3} mm/cycle, the influence of R is nearly absent between $R = 0.2$ and 0.4.

Figs. 2(b) and 2(c) show the da/dN − ΔK plots for $B = 12$ and 24 mm, respectively. For $B = 12$ mm, Fig. 2(b) shows that the same behavior is observed for $B = 6$ and 12 mm. However, the influence of R on da/dN is less pronounced, and becomes virtually absent for da/dN close to 10^{-3} mm/cycle and still $\Delta K = 50$ MPa m$^{-1/2}$.

While the mean stress effect for $B = 24$ mm can be observed in Fig. 2(c), it is not as significant as than for $B = 6$ and 12 mm.

Fig. 3(a) shows the influence of specimen thickness on crack growth for $R = 0$. It can be seen that da/dN increases with thickness. This effect becomes less significant as ΔK increases; it is more pronounced between $B = 6$ and 12 mm than between $B = 12$ and 24 mm.

The plots of da/dN − ΔK obtained for the other stress ratios $R = 0.2$ and 0.4 show similar trends but with less influence of B on da/dN.

3.2. Opening load stress intensity factor

Since fatigue crack growth rate has shown a strong dependence on both stress ratio and specimen thickness, a crack closure analysis was carried out to correlate the results with ΔK_{eff} initially proposed in Ref. [3]. A typical plot of the crack

Table 3
Models to estimate U

Material	Reference	Model
2024–T3 Al	[3]	$U = 0.5 + 0.4R, \quad 0.1 < R < 0.7$
2024–T3 Al	[8]	$U = 0.55 + 0.35R + 0.1R^2, \quad \alpha = 0.1$
Titanium	[9]	$U = \frac{1}{1-R}\left[1 - \frac{6.67R - 4.27}{K_{max}}\right]$
6063–T6 Al	[10]	$U = \left(\frac{13.5R + 5.925}{1000}\right)\Delta K + 1.35R + 0.223$
Mild steel	[15]	$U = 0.7 + 0.15R(2 + R)$
Steel	[16]	$U = 0.75 + 0.25R$

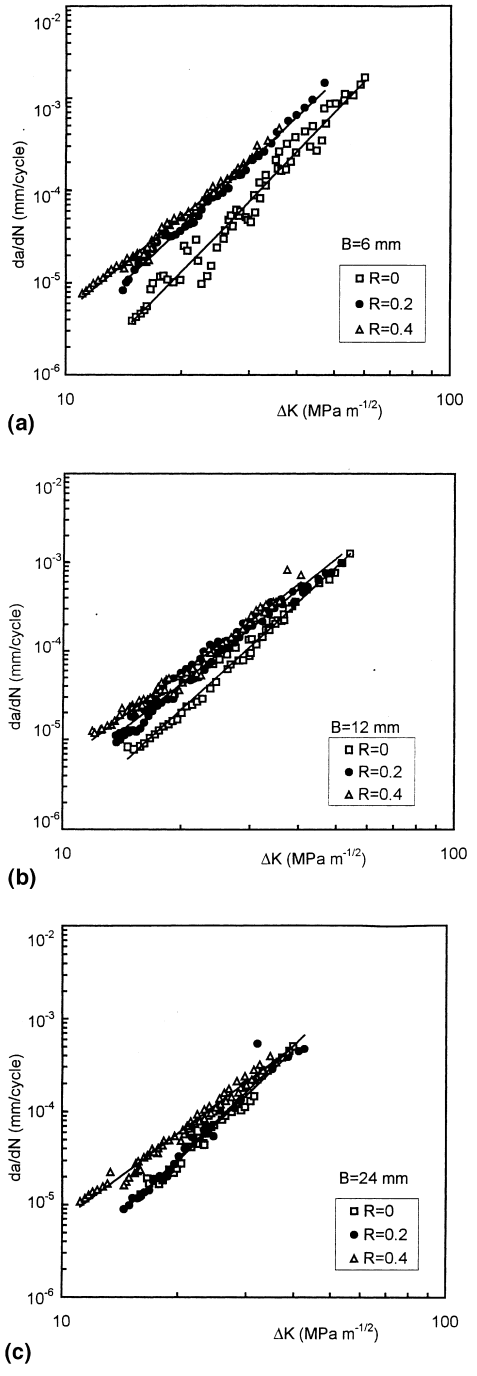

Fig. 2. da/dN versus ΔK curves for $R=0$, 0.2 and 0.4: (a) $B=6$ mm; (b) $B=12$ mm; (c) $B=24$ mm.

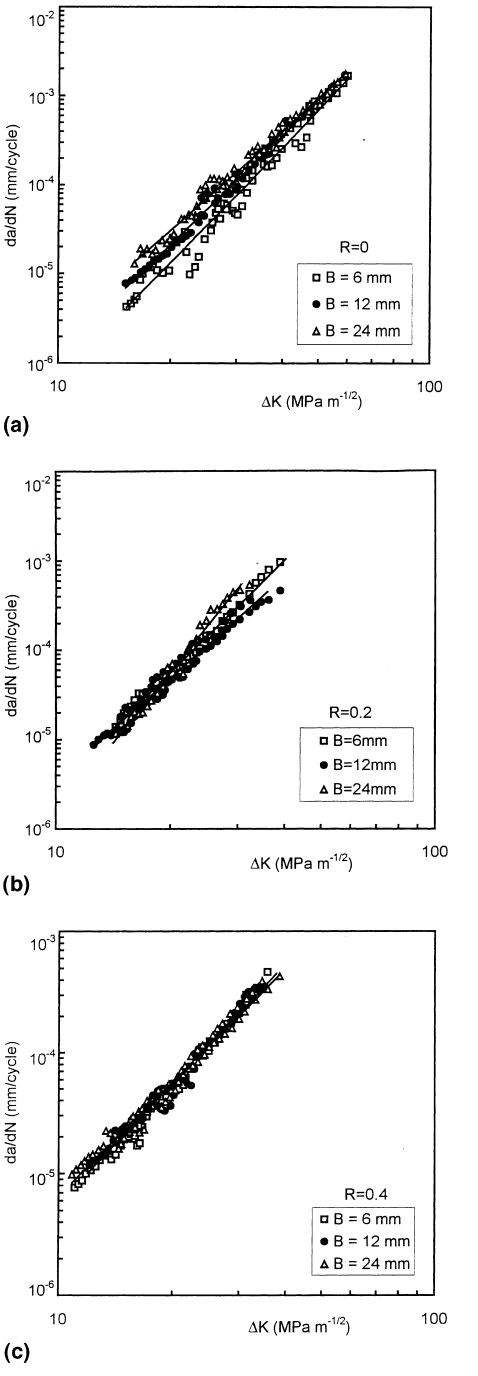

Fig. 3. da/dN versus ΔK curves for $B=6$, 12 and 24 mm: (a) $R=0$; (b) $R=0.2$; (c) $R=0.4$.

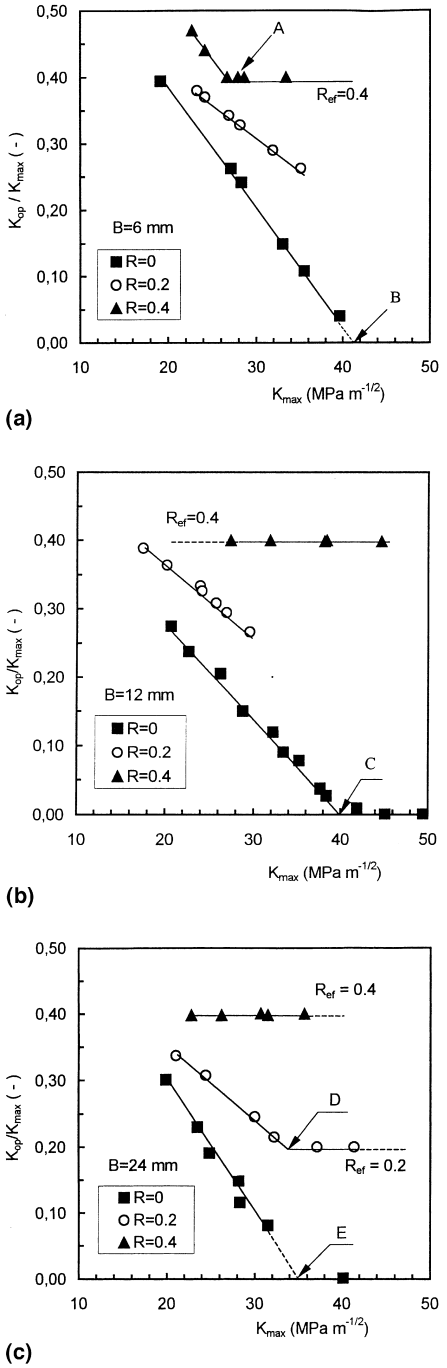

Fig. 4. K_{op}/K_{max} versus K_{max}, for $R=0$, 0.2 and 0.4: (a) $B=6$ mm; (b) $B=12$ mm; (c) $B=24$ mm.

opening load obtained with the clip gauge was shown in Fig. 1, where P_{op} is the opening load.

Fig. 4(a)–(c) present the variations of K_{op}/K_{max} with K_{max} for $B=6$, 12 and 24 mm, respectively. All these plots are compared with the three values of the stress ratios $R=0$, 0.2, and 0.4. The points indicated in Figs. 4 and 5 represent values of K_{max} above which $K_{op}/K_{max}=R$. Numerical results are given in Table 4. Fig. 4(a) (for $B=6$ mm) shows that K_{op}/K_{max} decreases as K_{max} increases until the minimum value K_{op}/K_{min} was attained, where $R_{eff}=R$. For example at point A, where $K_{max}=28$ MPa $m^{-1/2}$, $K_{op}<K_{min}$, and $R_{eff}=R=0.4$. For $R=0.2$, the condition $R_{eff}=R$ can be obtained only for $K_{max}\approx 40$ MPa $m^{-1/2}$. From the trend of the curve for $R=0$, $R_{eff}=R$ is estimated to occur at point B for $K_{max}\approx 40$ MPa $m^{-1/2}$.

Fig. 4(b) shows that for $B=12$ mm and $R=0.4$, crack closure measurements could not be obtained even for the lower values of K_{max}. However, for $R=0.2$, K_{op}/K_{max} decreases as K_{max} increases. Points C corresponds to $K_{max}=40$ MPa $m^{-1/2}$, above which the ratio K_{op}/K_{max} becomes constant and equals to $R=0$.

The results in Fig. 4(c) for $B=24$ mm are similar to those for other thicknesses. Crack closure was not observed for $R=0.4$. For the others stress ratios, K_{op}/K_{max} tends to a lower limit defined by the stress ratio R, after which K_{op}/K_{max} remains constant. Such a behavior is shown for $R=0.2$ for point D at $K_{max}=34$ MPa $m^{-1/2}$ and $R=0$ for point E at $K_{max}=36$ MPa $m^{-1/2}$

From the results plotted in Fig. 4(a)–(c), it can be concluded that:

- for $R=0.4$, the values of K_{op} are higher than K_{min} only for lower thickness of $B=6$ mm and for $K_{max}<28$ MPa $m^{-1/2}$. No crack closure was observed for the other thicknesses $B=12$ and 24 mm, and therefore $R_{eff}=R$ in the range of K_{max} values was analyzed;
- for $R=0$ and 0.2, K_{op}/K_{max} decreases as K_{max} increases until the minimum value was attained where $R_{eff}=R$;
- the ratio K_{op}/K_{max} is lower for the lower stress ratios;
- the condition $K_{op}/K_{max}=1$ was attained for K_{max} values that increases as R decreases, since R is positive.

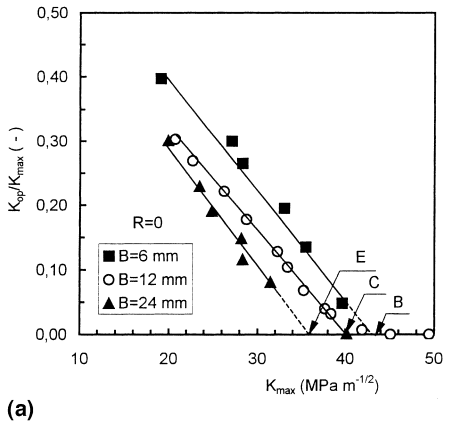

(a)

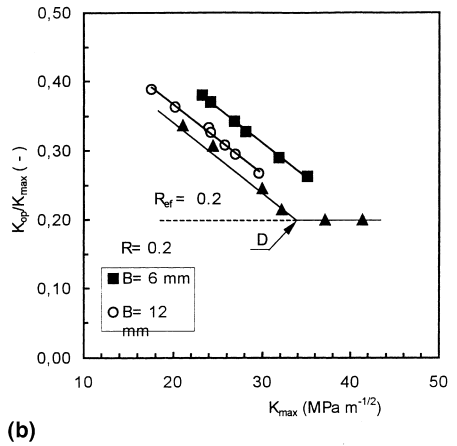

(b)

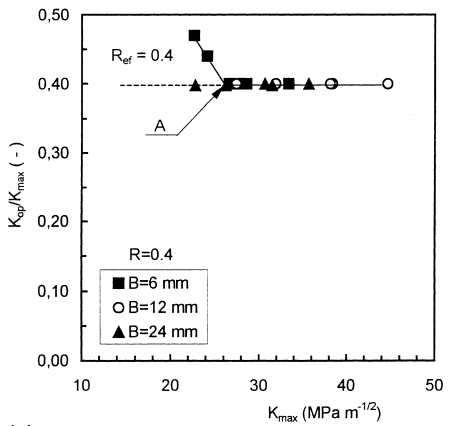

(c)

Fig. 5. K_{op}/K_{max} versus K_{max}, for $B=6$, 12 and 24 mm: (a) $R=0$; (b) $R=0.2$; (c) $R=0.4$.

Table 4
Key points on the curves K_{op}/K_{max} – K_{max} above which $K_{op}/K_{max}=R$

Point	R	B	ΔK (MPa $m^{-1/2}$)	K_{max} (MPa $m^{-1/2}$)
A	0.4	6	16.8	28
B	0	6	42	42
C	0	12	40	40
D	0.2	24	27.2	34
E	0	24	36	36

Plotted in Fig. 5(a)–(c) are, respectively, the results of K_{op}/K_{max} against K_{max} for different stress ratio of $R=0$, 0.2 and 0.4. Three different specimen thicknesses of $B=6$, 12 and 24 mm are covered. The behavior observed for $R=0$ and 0.2 in Fig. 5(a) and (b) is similar. The influence of specimen thickness on crack represented by K_{op}/K_{max} is highest for $B=6$ mm. In Fig. 5(a), point E corresponds, to $K_{max}=36$ MPa $m^{-1/2}$ (for $B=24$ mm) above which $R_{eff}=0$. Point C corresponds to $K_{max}=40$ MPa $m^{-1/2}$ (for $B=24$ mm) above which $R_{eff}=0$. The curves in Fig. 5(c) pertain to $R=0.4$. Crack closure is observed only for $B=6$ mm and K_{max} below 28 MPa $m^{-1/2}$. For $B=12$ and 24 mm, the values of K_{op} are below K_{min}. Therefore, for $K_{max} > 28$ MPa $m^{-1/2}$ there is no influence of specimen on crack closure for this stress ratio.

3.3. Normalized load ratio parameter

Other forms of crack closure data can be represented by plotting the normalized load ratio parameter U defined by Eq. (1) as a function of ΔK. Fig. 6 shows that U tends to increase with ΔK for $B=6$ mm and all values of R. For $\Delta K > 16$ MPa $m^{-1/2}$ and $R=0.4$, U takes a constant value of unity. Curves for $B=12$ and 24 mm are not shown; their trends are similar to those in Fig. 6 except that the effect of R is less pronounced.

Displayed in Fig. 7 are variations of U versus ΔK for $R=0$. For a given ΔK, U increases with the specimen thickness. Note that points E and C correspond to $U=1$ for $B=24$ mm ($\Delta K=36$ MPa $m^{-1/2}$) and $B=12$ mm ($\Delta K=40$ MPa $m^{-1/2}$), respectively. The data for $R=0.2$ and 0.4 mm are similar but not shown.

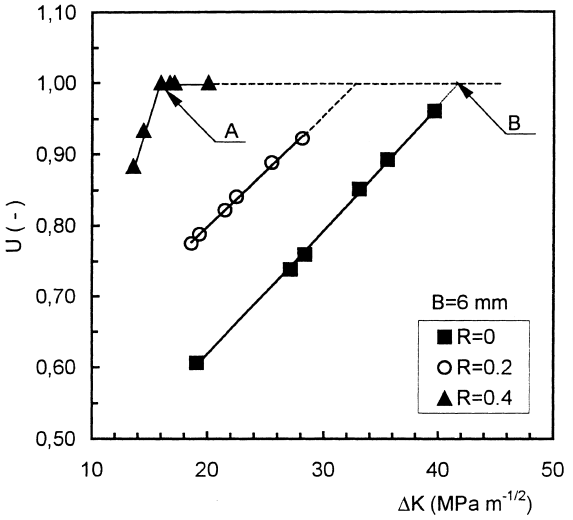

Fig. 6. U versus ΔK, $B=6$ mm, $R=0$, 0.2 and 0.4.

3.4. Effective stress intensity factor

The change of effective stress intensity factor ΔK_{eff} can be calculated from U and ΔK according to Eq. (3). The objective is to represent the crack closure data by a single curve independent of R or B.

From the values of U calculated, the curves da/dN – ΔK_{eff} were derived. The objective is to analyze if the crack closure by itself reduces all the da/dN – ΔK curves at a unique curve of da/dN – ΔK_{eff} independent R or B.

Fig. 8 shows these results for the three stress ratios and thicknesses. All results tend to fall within a width for all values of R or B when da/dN is plotted against ΔK_{eff} according to

$$\mathrm{d}a/\mathrm{d}N = 2 \times 10^{-8} \Delta K_{\text{eff}}^{2.7468}. \tag{4}$$

The correlation factor is 0.98.

The models of U shown in Table 3 present this parameter as a function of R only or of R and ΔK or $K_{\max}$. However, this work showed that the thickness can also have an important effect on crack closure. Presented in Eq. (5) is an expression that relates U to R, ΔK and B by using a multiple linear regression:

$$\begin{aligned} U &= 0.716R + 0.012\Delta K + 0.144(\mathrm{B/W}) \\ &\quad + 0.433 \quad \text{if} \quad \beta < 0.567, \\ U &= 1 \qquad\quad \text{if} \quad \beta > 0.567, \end{aligned} \tag{5}$$

where

$$\beta = 0.716R + 0.0121\Delta K + 0.144(\mathrm{B/W}). \tag{6}$$

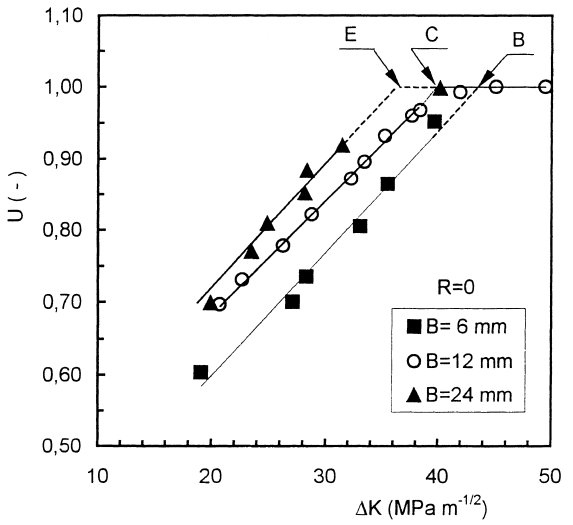

Fig. 7. U versus ΔK, $R=0$, $B=6$, 12 and 24 mm.

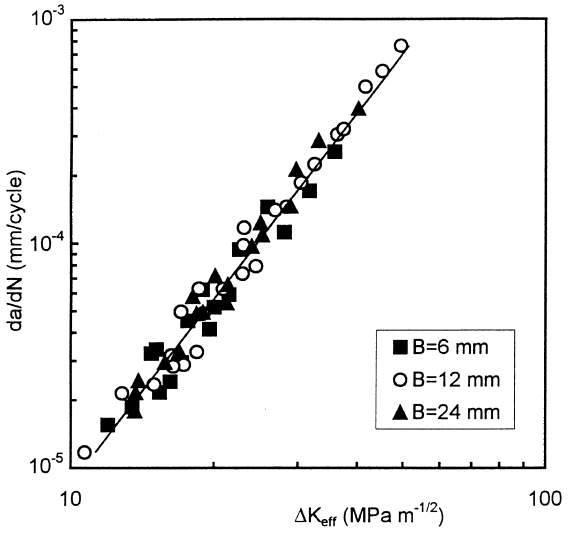

Fig. 8. da/dN versus ΔK_{eff}, for $R=0$, 0.2 and 0.4 and $B=6$, 12 and 24 mm.

Although the correlation factor 0.941 is low, this equation can be used for the determination of U in for CK steel in the range for $0 < R < 0.4$ and $6 < B < 24$ mm.

The validation of this equation was analyzed by plotting da/dN as a function of the values of ΔK_{eff}. Fig. 9 shows these results for the three stress ratios and thicknesses. A continuous band is obtained that appears to be appropriate for determining the influence of R and B on U.

Proposed in Ref. [3] using U from Eq. (5), it can be stated that

$$da/dN = 9 \times 10^{-9} \Delta K_{eff}^{2.95}. \quad (7)$$

The difference of the values of C and m constants between Eqs. (4) and (7) are due to the use of $da/dN - \Delta K$ data calculated from Eq. (5) for obtaining Eq. (7), while Eq. (4) is found from the experimental data for da/dN and ΔK.

4. Conclusions

1. A strong influence of both stress ratio R and specimen thickness B on the fatigue crack growth was observed for the CK45 steel. da/dN increases with R or B. The influence of specimen thickness is more pronounced for the lower stress ratio $R = 0$. The influence of R and B on da/dN tends to decrease as ΔK increases while da/dN is more sensitive to change of R for the lower thickness range.

2. Crack closure data were obtained and plotted for $R_{eff} = K_{op}/K_{max}$ versus K_{max}. As K_{max} increases R_{eff} decreases until the $R_{eff} = R$ condition was attained. K_{op}/K_{max} decreases with R. No crack closure was observed for $R = 0.4$ except for the lowest specimen thickness $B = 6$ mm. For constant stress ratio R, R_{eff} increases as the specimen thickness decreases.

3. The crack closure load parameter U was also determined and plotted versus ΔK. It increases with R and B. The influence of R on U is more strong for the lowest thickness $B = 6$ mm. Also, the influence of B on U is stronger for $R = 0$ than for $R = 0.2$ and is virtually insignificant for $R = 0.4$.

4. Despite some scatter obtained for the curves $da/dN - \Delta K_{eff}$ the results for the three stress ratios and thicknesses are represented by a single curve for the two-parameter crack growth rate relation as applied to the CK45 steel.

5. A model of U as function R, B and ΔK was proposed based on the experimental crack closure data. This model is limited to $0 < R < 0.4$ and $6 < B < 24$ mm.

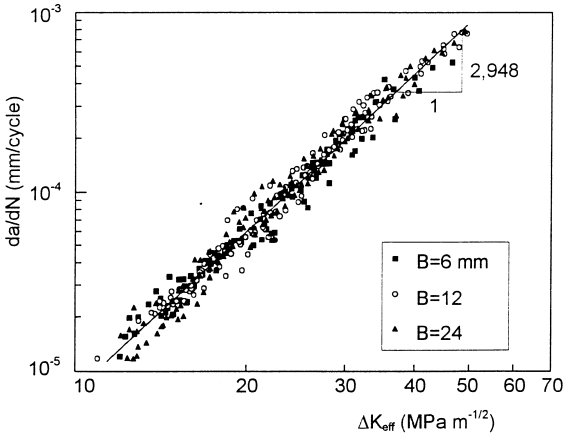

Fig. 9. da/dN versus ΔK_{eff}, using the model of U (Eq. (5)). $R = 0$, 0.2 and 0.4, and $B = 6$, 12 and 24 mm.

References

[1] W. Elber, Fatigue crack closure under cyclic tension, Eng. Fract. Mech. 2 (1970) 37–45.
[2] A.F. Blom, D.K. Holm, An experimental and numerical study of crack closure, Eng. Fract. Mech. 22 (1984) 997–1011.
[3] W. Elber, The significance of fatigue crack closure, ASTM STP415 (1971) 230–242.
[4] J. Schijve, Tour lectures on fatigue crack growth, Eng. Fract. Mech. 11 (1979) 167–221.
[5] O.N. Romaniv, A.N. Track, Y.N. Lenets, Effects of fatigue crack closure on near threshold crack resistance on structural steels, Fat. Fract. Eng. Mat. Struct. 10 (1987) 263–272.
[6] N.C. Lafarie-Frenot, J. Petit, C. Gasc, A contribution to the study of fatigue crack closure in vacuum, Fat. Eng. Mat. 1 (1979) 431–438.
[7] R.O. Ritchie, Slow crack growth macroscopic aspects, in: R.B. Tait, G.G. Garret (Eds.), Proceedings of the 2nd National Conference on Fracture, University of Witwatersrand, Johannesburg, Pergamon Press, Oxford, 1984.

[8] J. Schijve, Some formulas for crack opening stress level, Eng. Fract. Mech. 14 (1981) 461–465.
[9] V. Bachmann, D. Munz, Crack closure in fatigue of titanium alloy, Int. J. Fract. 11 (1975) 713–716.
[10] Y.P. Srivastava, S.B.L. Garg, Influence of R on effective stress range ratio and crack growth, Eng. Fract. Mech. 22 (1985) 915–926.
[11] K.D. Unangst, T.T. Shih, R.P. Wei, Crack closure in 2219-T851 Al-alloy, Eng. Fract. Mech. 9 (1977) 725–734.
[12] N.J.I. Adains, Fatigue crack closure at positive stresses, Eng. Fract. Mech. 4 (1972) 543–554.
[13] H. Bao, A.J. McEvely, The effect of thickness on the rate of fatigue crack growth, in: G. Lutjering, Nowack (Eds.), Proceedings of the 6th International Fatigue Congress, Berlin, Germany, Pergamon Press, Oxford, 1996, pp. 381–386.
[14] Standard test method for constant-load-amplitude fatigue crack growth rates above 10-8 m/cycle, ASTM E 647-86 (1987) 765–783.
[15] R. Kumar, K. Singh, Influence of stress ratio on fatigue crack growth in mild steel, Eng. Fract. Mech. 50 (1995) 377–384.
[16] S.J. Madox, T.R. Curney, A.M. Mummey, G.S. Booth, An investigation of the influence of applied stress ratio on fatigue crack propagation in structural steels, Research Report 72/1978, Welding Institute, 1978.